F. Soniak and L. Remy**

Fatigue Growth of Long and Short Cracks in a Powder Metallurgy Nickel Base Superalloy

REFERENCE Soniak, F. and Remy, L., **Fatigue Growth of Long and Short Cracks in a Powder Metallurgy Nickel Base Superalloy**, *The Behaviour of Short Fatigue Cracks*, EGF Pub. 1 (Edited by K. J. Miller and E. R. de los Rios) 1986, Mechanical Engineering Publications, London, pp. 133–142.

ABSTRACT Some aspects of the differences in fatigue crack growth behaviour and threshold data, for long and short cracks, are presented in this paper. Tests were carried out at room temperature on a H.I.P. + forged Astroloy, which has a necklace structure. For long cracks, closure is found to depend upon the stress ratio, but is independent of crack length and the maximum stress intensity factor. Short cracks were found to grow faster than long cracks. The influence of crack length on fatigue crack growth rate has been rationalized using the effective range of the stress intensity factor, and a unique intrinsic crack growth law is proposed for long and short cracks.

Introduction

Powder metallurgy superalloys are currently being developed for turbine disc applications in advanced turbine engines. However, defects are inherent to this manufacturing process and they can initiate short cracks under fatigue cycling. An accurate prediction of fatigue life is needed for aeroengine components. Generally, life calculations are made by the integration of the Paris law (**1**): $da/dN = C(\Delta K)^m$, from the largest size of initial defect to the crack length at final fracture. But the growth rate of short cracks (**2**)(**3**), and of long cracks at high stress ratios (**4**)(**5**) is faster than that of long cracks, say about 5 mm, at low stress ratios, which are generally used in laboratories to characterize fatigue crack growth behaviour. It follows that the use of the 'defect tolerant' approach with such laws leads to non-conservative predictions of the fatigue lives of components. This work reports on the influence of the stress ratio R and crack length upon fatigue crack growth rate in a powder metallurgy nickel base alloy, at room temperature. The aim of this work was to find a common parameter for all the crack configurations, which could rationalize any difference in fatigue crack growth behaviour and lead to conservative fatigue life predictions.

Fatigue crack growth rate results are reported here for long cracks, using CT and SEN specimens, together with crack closure measurements for various stress ratios. Short crack growth rate data are then presented for artificial short through-cracks. Differences in behaviour between short and long cracks are discussed using crack closure measurements.

* Centre des Matériaux de l'Ecole des Mines de Paris, UA CNRS 866, B.P. 87–91003 Evry Cédex, France.

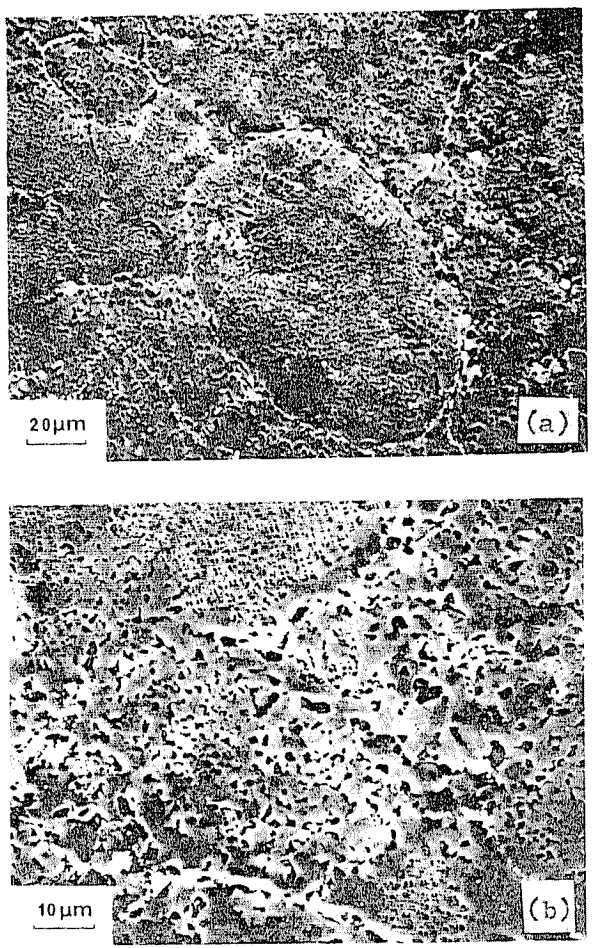

Fig 1 Microstructure of the coarse grain (a) and of the necklace structure (b) of the H.I.P. + forged Astroloy

Material and experimental procedure

The H.I.P. + forged Astroloy studied here has a necklace structure which is shown in Fig. 1, composed of coarse grains about 50 μm, and fine grains about 2 μm in diameter. The nominal percentage composition by weight is 0.022C, 0.003S, 14.8Cr, 5.04Mo, <0.01Cu, 16.9Co, 3.52Ti, 0.044Zr, 3.98Al, and 0.02B. The 0.2 per cent proof strength and ultimate tensile strength at room temperature are 1110 and 1510 MN . m^{-2}, respectively.

Long and short fatigue crack propagation studies were carried out at room

temperature in laboratory air. The fatigue tests were conducted on a servo-hydraulic fatigue testing machine using sine wave loading in the frequency range 30–60 Hz.

The growth rates of long fatigue cracks were measured on compact tension specimens 40 mm in width and 8 mm in thickness. A load shedding procedure was adopted for the threshold measurement on these specimens, using a 5–10 per cent decrease in load after a growth of 0.5 mm, down to about 5.10^{-11} m/cycle. Four stress ratios were investigated 0.1, 0.5, 0.7, and 0.9. The growth rate measured under the ΔK decreasing procedure were found to be in agreement with those measured under constant load at increasing fatigue crack growth rates.

Tests were also carried out down to the threshold under a stress ratio of 0.1 on single edge notched specimens 18 mm wide and 4 mm thick (Fig. 2(a)). Cracks were grown about 2 mm ahead of the notch in SEN specimens using the same load shedding procedure as in CT specimens. These SEN specimens were then machined down to about 12 mm in width and 2 mm in thickness (Fig. 2(b)). These machined SEN specimens contain a rectangular profile through-crack of 2mm in width and about 0.25–0.4 mm in depth. No heat treatment was given in order to prevent any modification of the crack surface. The plasticity left after all previous operations was kept to a minimum due to the threshold procedure adopted and the very cautious machining of specimens. The tests on these machined specimens were conducted at constant load, or using an increasing load procedure with steps of 5 per cent if crack growth did not occur after 10^6 cycles.

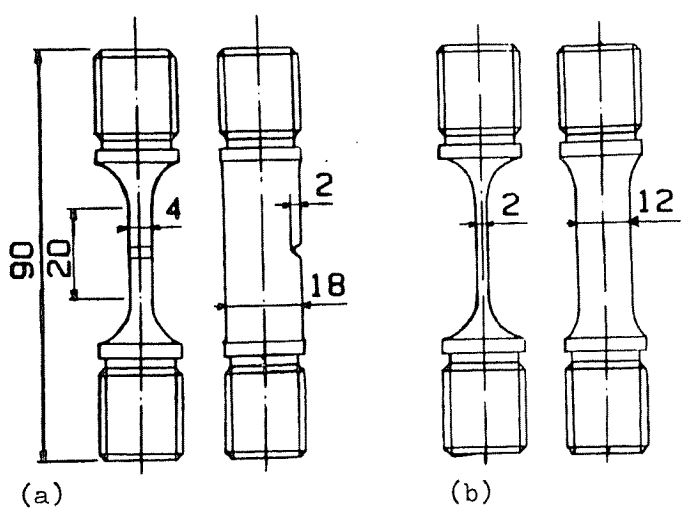

Fig 2 Single edged notched specimen geometry (in mm). (a) initially, (b) after machining to leave only a short crack

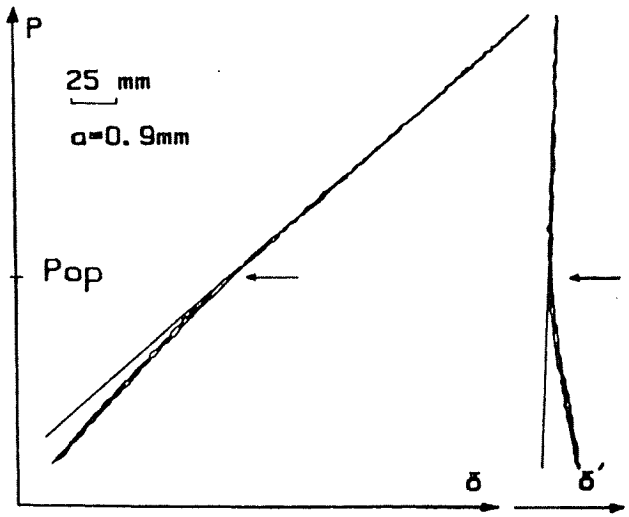

Fig 3 Experimental load–displacement curve

Crack growth was monitored using optical measurements on both sides of the specimen, also by a potential drop technique, and finally by a clip gauge extensometer located on the front part of the specimen. Load–displacement (P–δ) curves were recorded periodically at low frequency (0.5 Hz). The crack opening load P_{op} was determined by the upper break of the loading P–δ curve, which indicated that the crack was fully open (**6**). The opening load was more accurately measured using a corrected displacement $\delta' = \alpha P - \delta$ where α is an adjustable constant which was given by an electronic processor. One of the experimental curves is shown in Fig. 3 for a crack length of 0.9 mm. The value of P_{op} was quite difficult to assess but the evolution of the load displacement curve was so regular that the accuracy level was estimated to be about 10 per cent. The stress intensity factor at crack opening K_{op} was deduced from the opening load using the calibration formula for the relevant specimen geometry.

Experimental results

Long cracks

The results of the crack propagation tests using long cracks are reported in Fig. 4. The fatigue crack growth rates are reported on Fig. 4(a), as a function of the stress intensity range ΔK, for two specimen geometries (CT and SEN specimens), and four stress ratios (0.1, 0.5, 0.7, and 0.9). The threshold stress intensity range ΔK_{th} was conventionally defined for a crack growth rate of 10^{-10} m/cycle. The ΔK_{th} value decreases from about 10.5 MPa$\sqrt{m}$ to about 3 MPa$\sqrt{m}$ when the stress ratio increases from 0.1 to 0.9. The same fatigue crack growth data are reported in Fig. 4(b) versus the effective stress intensity range

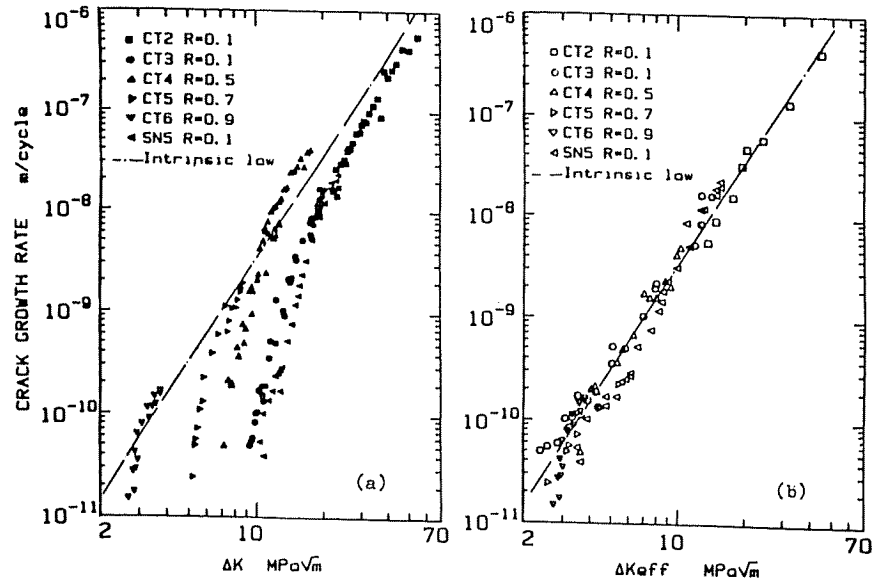

Fig 4 Fatigue crack growth rates of long cracks at different load ratios. (a) versus ΔK; (b) versus ΔK_{eff}

ΔK_{eff}, defined as $K_{max} - K_{op}$. All the results fit a single straight line within a small degree of scatter from the low rate region to the high rate region, i.e., in the range 5.10^{-11}–10^{-6} m/cycle. The stress ratio dependency of FCGR has completely disappeared when using ΔK_{eff}, by accounting for the crack closure phenomenon. The value of the opening stress intensity factor K_{op} has been plotted versus the maximum stress intensity factor K_{max} and the normalized crack size a/W, respectively, in Fig. 5(a) and (b). For each stress-ratio, 0.1, 0.5, and 0.7 the K_{op} value seems to be a constant for these long cracks. By increasing the stress ratio from 0.1 to 0.7 the K_{op} value increases from 8.3 to 14.9 MPa$\sqrt{m}$.

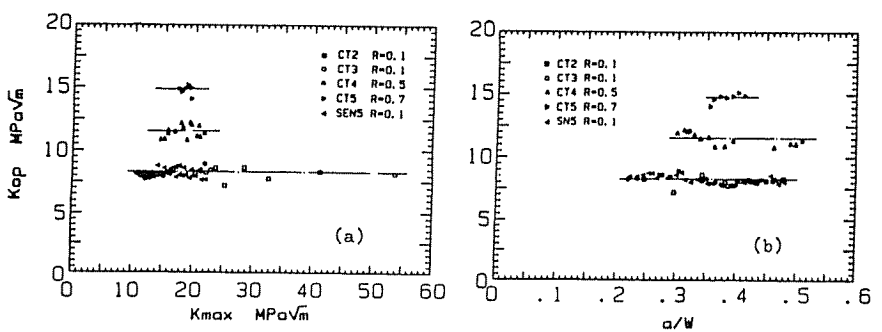

Fig 5 Crack opening stress intensity factor K_{op} of long cracks as a function of (a) K_{max}, (b) the normalized crack size, a/W

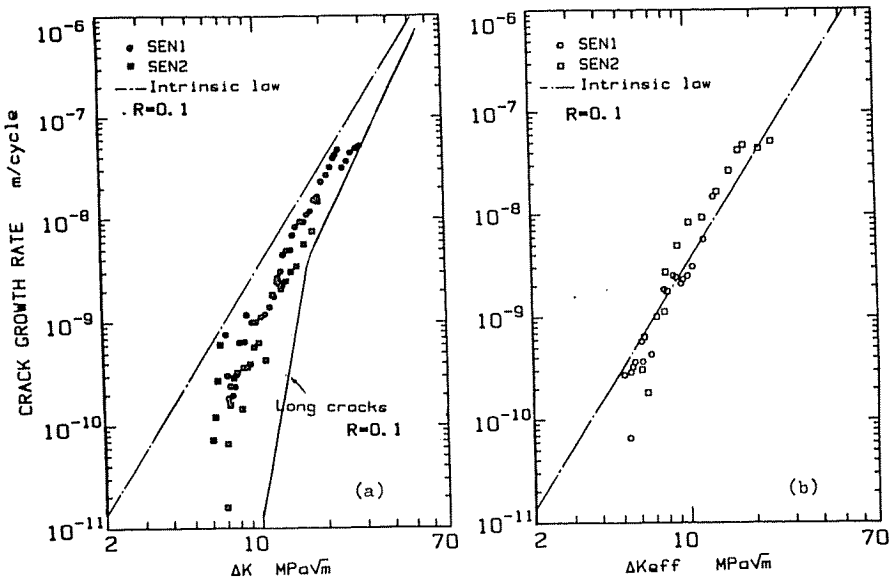

Fig 6 Fatigue crack growth rates for short cracks. (a) versus ΔK; (b) versus ΔK_{eff}

Short cracks

Fatigue crack growth rates of short cracks are reported as a function of the stress intensity range ΔK in Fig. 6(a) for a stress-ratio of 0.1. It can be seen that short cracks are able to propagate below the long crack threshold stress intensity and at a crack growth rate more than thirty times that of long cracks. The results are plotted versus the effective stress intensity range ΔK_{eff} in Fig. 6(b). As for long cracks all the results are along a single straight line which is similar to that for long cracks. The K_{op} values are reported versus ΔK and the crack size a, in Fig. 7(a) and (b) respectively. The value of K_{op} increases with crack size and merges with the long crack data at a value of 8.3 MPa$\sqrt{m}$ at crack sizes ranging from 2 to 3 mm. The K_{op} value has been found to increase also with increasing ΔK values up to a value of 20 MPa$\sqrt{m}$.

Discussion

From the present results it is clear that the range of the stress intensity factor alone cannot account for stress ratio and crack size effects on fatigue crack growth rate, as seen by previous authors (**7**)–(**12**). Many authors since Pearson (**2**) have studied the growth of natural cracks in smooth specimens. Assumptions must be made to calculate the fatigue crack growth rate and also the stress intensity range ΔK (**13**). For example, many studies use observations of cracks

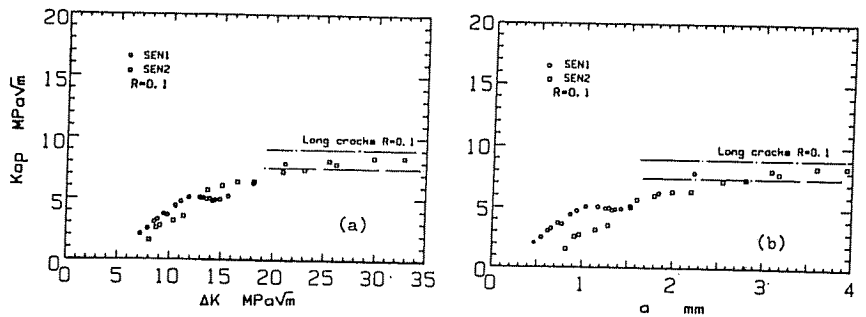

Fig 7 Crack opening stress intensity factor K_{op} of short cracks as a function of (a) ΔK, (b) the crack length, a

on the specimen surface and the assessment of crack shape and depth relies upon a calibration curve which is established from broken specimens. Such data are not easily generated for the smaller crack sizes, and the accuracy of the calibration curve becomes questionable. Natural cracks initiate generally at material inhomogeneities (**10**)–(**14**) such as inclusions, pores, and second phase particles. When the crack is much larger than the size of the initiation defect it has an equilibrium shape and the calibration curve should apply. However this becomes questionable at short crack lengths where defects are at or near the outer surface where cracks may not be of equilibrium shape (**15**). Furthermore short crack behaviour near the initiating defect can be influenced by local stress concentrations (at pores or inclusions) and residual stress patterns inherited from the manufacture process due to inclusions, second phase particles, etc. Finally in the whole range of crack sizes, natural cracks involve a three-dimensional fracture mechanics problem and the variation of the stress intensity factor along the crack front has to be taken into account.

On the other hand, the artificial short cracks as described here, may be accurately described as two dimension through-cracks. The assumptions made, concerning bidimensionality and a uniform stress intensity factor along the crack front are realistic in this case. The artificial short cracks, as used in the present work, are a convenient way to study the crack length dependency of fatigue crack growth behaviour, even though natural cracks are more representative of situations occurring in real components.

As seen in Fig. 5(b) the opening stress intensity factor K_{op} is equal to about 8.3 MPa$\sqrt{m}$ for a stress ratio of 0.1 for long cracks (>3 mm) and for two specimens geometries (CT and SEN). In Fig. 7(b) the K_{op} value of short cracks increases from zero for crack sizes ranging from 0.2 to 0.5 mm, and merges with the long crack K_{op} value for crack sizes ranging from 2 to 3 mm. We estimated the length of the crack faces which 'close' during unloading to the minimum load, from measurements of the compliance change associated with closure. We took care of any underload effect and we unloaded specimens to the

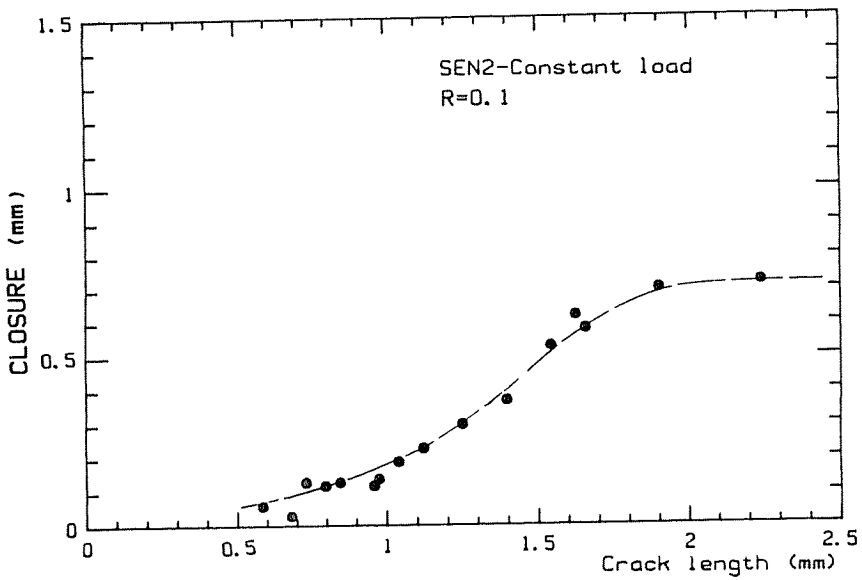

Fig 8 Length of closure in wake versus crack length

minimum load. So when the crack is closed, the measured compliance provides an apparent crack length from graphs of compliance against crack length. This has been done previously by James and Knott (**16**) and for cracks in this study (Fig. 8). In this figure the closed crack length in the wake is plotted against the crack length. It should be emphasized that these data refer to crack growth under increasing ΔK. As seen by James and Knott the length of the closure in the wake increases from about zero for a crack size of 0.5 mm and stabilizes at about 0.7 mm for a crack size of 1.5 mm when ΔK is increasing. As seen in Fig. 5(b), for long cracks the K_{op} value is constant whatever the crack size. For the CT specimens, the closure in the wake was observed to be identical to the real crack length ahead of the notch (**17**); this behaviour was observed for specimens tested under a load shedding procedure (i.e., at decreasing ΔK) as well as for specimens tested under constant load (i.e., at increasing ΔK). On the other hand, for the long cracks studied on SEN specimens (4 mm in thickness), the closure in the wake was always smaller than the crack length using a load shedding procedure. A constant K_{op} value was observed for long cracks for both CT and SEN specimens, using either a decreasing ΔK or an increasing ΔK procedure. However, this constant K_{op} behaviour corresponds to very different closure behaviours in the wake and so the opening stress intensity factor K_{op} is not simply connected to the closure in the wake for this material nor the slightly different closure stress intensity factor.

The crack length dependency of K_{op} and of the closure in the crack wake observed for an artificial short crack suggests that a minimum closure in the wake is required to establish a stabilized crack opening stress intensity factor. In the present case the length of material behind the crack tip responsible for closure would be about 0.5–1 mm. This conclusion is in pretty good agreement with the electro discharge machining experiments of Minakawa *et al.* (**11**) on CT specimens which showed that most of the closure behaviour was due to material 1 mm behind the crack tip.

The fatigue crack growth rate of long cracks and short cracks are plotted versus the effective stress intensity range in Figs 4(b) and 6(b), respectively. All the data fit onto a single straight line within a small degree of scatter. A single intrinsic law at room temperature for this H.I.P. + forged Astroloy is observed whatever the crack length ($R = 0.1$) or the stress ratio of the long crack. Previously we saw that the closure phenomenon is associated with closure in the crack wake but we saw also that the closure in the wake is not connected with the K_{op} value. Crack closure should be dependent upon surface roughness in the present alloy, but other mechanisms could also be operative ignoring any environmental influence.

Conclusions

(1) The present investigation into the influence of stress ratio on long crack growth behaviour at room temperature in H.I.P. + forged Astroloy has shown that consideration of crack closure can normalize fatigue crack growth rate curves. This consideration leads to an intrinsic crack growth law of da/dN versus ΔK_{eff} for long cracks.

(2) Differences in fatigue crack growth rates between long and short cracks, at the same stress ratio of 0.1, have been shown to be the consequence of the crack length dependency of crack closure behaviour at short crack lengths. A unique intrinsic crack growth law, da/dN versus ΔK_{eff}, has been observed for long and short cracks. This law should lead to conservative predictions of fatigue crack growth life.

Acknowledgements

The authors are indebted to Turboméca for provision of research facilities and the DRET for financial support.

References

(1) PARIS, P. C., BURKE, J. J., REED, N. L., and WEISS, V. (1964) Fatigue, an interdisciplinary approach, *Proceedings of the 10th Sagamore Army Materials Research Conference* (Syracuse University Press), pp. 107–127.

(2) PEARSON, S. (1975) Initiation of fatigue cracks in commercial aluminium alloys and the subsequent propagation of very short cracks, *Engng Fracture Mech.*, **7**, 235–247.

(3) LANKFORD, J. (1977) Initiation and early growth of fatigue cracks in high strength steel, *Engng Fracture Mech.*, **9**, 617–624.

(4) KLESNIL, M. and LUKAS, P. (1972) Effect of stress cycle asymmetry on fatigue crack growth, *Mat. Sci. Engng*, **9**, 231–240.
(5) USAMI, S. (1982) Applications of threshold cyclic-plastic-zone-size criterion to some fatigue limit problem, *Fatigue Thresholds*, Edited by J. Bäcklund, A. F. Blom, and C. J. Beevers (EMAS), Vol. 1, pp. 205–238.
(6) ELBER, W. (1971) The significance of fatigue crack closure, *Damage tolerance in aircraft structures, ASTM STP 486* (American Society for Testing and Materials), pp. 230–242.
(7) KITAGAWA, H. (1982) Limitations in the applications of fatigue threshold ΔK_{th}, *Fatigue thresholds*, Edited by J. Bäcklund, A. F. Blom, and C. J. Beevers (EMAS), Vol. 2, pp. 1051–1068.
(8) NAKAI, Y., TANAKA, K., and NAKANISHI, T. (1981) The effects of stress ratio and grain size on near-threshold fatigue crack propagation in low carbon steel, *Engng Fracture Mech.*, **15**, 291–302.
(9) VENABLES, R. A., HICKS, M. A., and KING, J. E. (1984) Influence of stress ratio on fatigue thresholds and structure sensitive crack growth in Ni-base superalloys, *Fatigue crack growth threshold concepts*, Edited by D. Davidson and S. Suresh (T.M.S. AIME, Warrendale, Pennsylvania), pp. 341–357.
(10) SCHIJVE, J. (1982) Differences between the growth of small and large fatigue cracks in relation to threshold in *Fatigue thresholds*, Edited by J. Bäcklund, A. F. Blom, and C. J. Beevers (EMAS), Vol. 2, pp. 881–908.
(11) MINAKAWA, K., NEWMAN, J. C., Jr, and McEVILY, A. J. (1983) A critical study of the crack closure effect on near-threshold fatigue crack growth, *Fatigue Engng Mater. Structures*, **6**, 359–365.
(12) BREAT, J. L., MUDRY, F., and PINEAU, A. (1983) Short crack propagation and closure effects in A508 steel, *Fatigue Engng Mater. Structures*, **6**, 349–358.
(13) BROWN, C. W., KING, J. E., and HICKS, M. A. (1984) Effects of microstructure on long and short crack growth in nickel base superalloys, *Metal Sc.*, **18**, 374–380.
(14) CLEMENT, P., ANGELI, J. P., and PINEAU, A. (1984) Short crack behaviour in nodular cast iron, *Fatigue Engng Mater. Structures*, **7**, 251–265.
(15) FOTH, J., MARISSEN, R., NOWACK, M., and LUTJERING, G. (1984) A fracture mechanics based description of the propagation behaviour of small cracks at notches, *Proceedings of the 5th European Convention on Fracture*, Edited by L. Faria, pp. 135–144.
(16) JAMES, M. N., and KNOTT, J. F. (1985) An assessment of crack closure and the extent of the short crack regime in Q1N (HY80) steel, *Fatigue Fracture Engng Mater. Structures*, **8**, 177–191.
(17) SONIAK, F. and REMY, L. (1984) Centre des Matériaux, E.M.P., Evry, France, Unpublished results.